Magnetic, electrical, and small-angle neutron-scattering studies of possible long-range order in the pyrochlores $Tl_2Mn_2O_7$ and $In_2Mn_2O_7$

N. P. Raju and J. E. Greedan
Institute for Materials Research, McMaster University, Hamilton, Canada L8S 4M1

M. A. Subramanian
E. I. DuPont de Nemours & Co., Central Research & Development, Wilmington, Delaware 19880-0328

(Received 24 August 1993)

$Tl_2Mn_2O_7$ and $In_2Mn_2O_7$ show spontaneous magnetization around 121 K indicating magnetic phase transitions. The related pyrochlores $Y_2Mn_2O_7$ and $Lu_2Mn_2O_7$ also exhibit spontaneous magnetization at their respective magnetic transition temperatures around 17 K. However, neutron-scattering studies do not provide any evidence for long-range order but suggest reentrant spin-glass behavior. In view of this we have performed small-angle neutron-scattering (SANS) investigations on $Tl_2Mn_2O_7$ and $In_2Mn_2O_7$. SANS results substantiate the long-range magnetic ordering in $Tl_2Mn_2O_7$ as indicated by the magnetic behavior. Preliminary SANS data of $In_2Mn_2O_7$, while more ambiguous, are not inconsistent with the presence of long-range order. Effective paramagnetic and saturation magnetic moments of $Tl_2Mn_2O_7$ and $In_2Mn_2O_7$ indicate the presence of Mn^{3+} ions on the Mn^{4+} sublattice as do the measured lattice constants. The occurrence of ferromagnetic ordering in these materials at high temperatures has been attributed to the double exchange interaction between Mn^{3+} and Mn^{4+} spins.

I. INTRODUCTION

The two series of compounds $R_2Mn_2O_7$ (R = Dy–Lu, or Y) and (R = Tl or In) belong to the family of pyrochlores with a general formula $A_2B_2O_7$.[1] These compounds crystallize in the face-centered-cubic structure with a space group $Fd\bar{3}m$. There are eight formula units per unit cell. Metal atoms A and B are located on the sites 16*d* and 16*c*, respectively, and two kinds of crystallographically different oxygens occupy the 48*f* and 8*b* sites. The $A_2B_2O_7$ structure is built up of slightly distorted BO_6 octahedra and strongly distorted AO_8 cubes. Each of the metal atoms in these compounds forms a three-dimensional network of corner-sharing tetrahedra. Such an arrangement leads to a very high degree of magnetic frustration if the nearest-neighbor interactions are antiferromagnetic.[2]

Magnetic transitions were found for the semiconducting compounds $R_2Mn_2O_7$ (R = Dy–Lu,Y) in the temperature range 20–40 K, and were attributed to ferromagnetic ordering based upon the observation of positive Θ_p values and spontaneous magnetization.[3] In this series, $Y_2Mn_2O_7$ and $Lu_2Mn_2O_7$ have each one magnetic sublattice (Mn^{4+} is magnetic, Y^{3+} and Lu^{3+} are nonmagnetic) and therefore could be the simplest series members. A thorough study of $Y_2Mn_2O_7$ by means of heat capacity and neutron scattering provided no evidence for a long-range order[4] contrary to the indication of spontaneous magnetization in Ref. 3. Instead, the absence of a sharp λ-type anomaly in the magnetic specific-heat data, the nonrecovery of total expected magnetic entropy at the transition temperature, and the diffuse neutron magnetic scattering pointed to a spin-glass-like ordering. Also preliminary small-angle neutron-scattering (SANS) studies indicated the presence of ferromagnetic clusters of finite size in the temperature range 13–20 K.[5]

Recently, in an extended study, ac and dc magnetic susceptibilities and small-angle neutron scattering (SANS) of $Y_2Mn_2O_7$ and $Lu_2Mn_2O_7$ have been discussed.[6] The dc susceptibility of $Lu_2Mn_2O_7$ increases rapidly below about 17 K with a ZFC-FC divergence for an applied field of 3 G, with results very similar to $Y_2Mn_2O_7$. This divergence disappears at relatively higher fields of about 300 G. SANS data of these two materials will be compared with those of $Tl_2Mn_2O_7$ in Sec. III C.

At this stage it is of interest to mention the magnetic behavior of another related series of pyrochlores $R_2Mo_2O_7$ (R = Nd–Yb, or Y).[7] $Nd_2Mo_2O_7$ appears to order ferromagnetically at about 95 K, and a ferrimagnetic coupling develops between the Nd and Mo moments at low temperatures. $Sm_2Mo_2O_7$ and $Gd_2Mo_2O_7$ show spontaneous magnetization around 70 and 57 K, respectively. However, heat capacity studies showed that long-range order does not develop in these two materials.[8] Magnetic susceptibility, heat capacity and neutron diffraction results of $Y_2Mo_2O_7$ indicate a spin-glass transition at 18 K.[8–11] In this series, compounds with R = Tb, Dy, Ho, Er, and Yb also show somewhat similar behavior.[12]

$Tl_2Mn_2O_7$ shows apparent spontaneous magnetization around 117 K and undergoes a semiconducting to semimetallic transition around this temperature.[13] The ordering temperature of $In_2Mn_2O_7$ was reported as 132 K.[14] Even though the magnetic data suggest ferromagnetic transitions in $Tl_2Mn_2O_7$ and $In_2Mn_2O_7$, in view of the complex magnetic ordering in the series of compounds $R_2Mn_2O_7$ and $R_2Mo_2O_7$, we wanted to study the nature of magnetic ordering in these compounds more thoroughly. In this work we report magnetic, electrical

TABLE I. Summary of the preparatory conditions of the samples.

Sample	Temperature	Pressure (kbar)
$Tl_2Mn_2O_7$ (I)	850 °C/30 min	60
$Tl_2Mn_2O_7$ (II)	800 °C/30 min	60
$In_2Mn_2O_7$	850 °C/60 min	60

and, for the first time, SANS studies of $Tl_2Mn_2O_7$ and $In_2Mn_2O_7$.

II. EXPERIMENTAL

Attempts to prepare $Tl_2Mn_2O_7$ and $In_2Mn_2O_7$ using the moderate pressure methods (3 kbar) which were successful for the $R_2Mn_2O_7$ series[3] failed. Instead, high-pressure methods were necessary. Two samples of $Tl_2Mn_2O_7$, in different batches, and a sample of $In_2Mn_2O_7$ have been prepared by the following procedure: Stoichiometric quantities of the reactants Tl_2O_3 (99.99%, Aldrich), In_2O_3 (99.9%, Alfa Inorganics), and MnO_2 (Specpure, Johnson & Matthey) were thoroughly mixed together in an agate mortar. Mixtures of about 200 mg each were sealed in small Pt capsules and heated at high pressures in a tetrahedral anvil. The capsules were rapidly cooled down to room temperature before releasing the pressure. The details of the solid-state reaction are given in Table I for each sample. Powder x-ray-diffraction data obtained with a Guinier-Hägg focusing camera revealed that the samples formed are single phase. Lattice constants, determined by a least-squares method, are in very good agreement with the literature values[13,14] which are collected in Table II.

Electrical resistivity of the samples, in the form of polycrystalline pellets, was measured using the conventional four-probe method. Sample temperature was varied from room temperature down to liquid He temperature by taking advantage of the temperature gradient in a liquid-He dewar. A diode thermometer was placed very close to the sample with a good thermal contact for the temperature measurement. Magnetic data have been obtained from room temperature down to 5 K with a SQUID magnetometer (Quantum Design, San Diego).

SANS data were collected at the McMaster Nuclear Reactor using 4.75 Å neutrons which were obtained with a Be filter and a pyrolytic graphite monochromator. The detector is a 128×128 element two-dimensional position sensitive detector (PSD). The distance between sample and detector is 3.35 m and the detector provides useful data in the range $0.020\ \text{Å}^{-1}\leq Q\leq 0.15\ \text{Å}^{-1}$ where the wave vector $Q=4\pi\lambda^{-1}\sin(\theta)$, 2θ being the scattering angle. The finely powdered sample was placed in an Al can and sealed with an indium gasket under He exchange gas. The sample holder was attached to a closed cycle refrigerator which can regulate the temperature to ±0.1 K in the range 300–10 K. SANS data at different temperatures, above and below T_c, have been obtained with a collection time of 8–16 hours. The magnetic contribution to the total SANS intensity was obtained by subtracting the data of 300 K (where magnetic contributions are negligibly small) from each temperature data set.

III. RESULTS AND DISCUSSION

A. X-ray-diffraction-unit cell constants

In Fig. 1 are compared the cubic cell constants of the $Tl_2Mn_2O_7$ and $In_2Mn_2O_7$ compounds with those of the $R_2Mn_2O_7$ series, R = Dy to Lu and Y, as a function of trivalent ion radius.[15] It is clear that for both materials the unit cell constants are significantly greater than the expected values based on the trend established for the $R_2Mn_2O_7$ series. There is evidence that members of this latter series, which can be prepared at the moderate pressure of 3 kbar, are stoichiometric.[3] The most likely cause of the increased cell constants is a small admixture of Mn^{3+} due to incomplete oxidation, i.e., an oxygen deficiency, $Tl_2Mn_2O_{7-x}$. The ionic radius of Mn^{3+}, 0.645 Å, is significantly greater than that of Mn^{4+}, 0.530 Å.[15] Further evidence for this model is found in the magnetic and electric transport data in Sec. III B and III C.

TABLE II. Values of the lattice constants, room-temperature resistivities, and effective paramagnetic moments for the samples of $Tl_2Mn_2O_7$ and $In_2Mn_2O_7$.

Sample	Lattice constant (Å)	Resistivity at RT (Ω cm)	Effective moment[a] (μ_B/Mn^{4+})
$Tl_2Mn_2O_7$ (sample 1)	9.889(1)	~1.3	3.96
$Tl_2Mn_2O_7$ (sample 2)	9.892(1)	~0.1	3.96
$Tl_2Mn_2O_7$ (Ref. 13)	9.890(3)	~13.0	4.1
$In_2Mn_2O_7$	9.727(1)	~10^4	3.77
$In_2Mn_2O_7$ (Ref. 14)	9.717		

[a]Effective magnetic moment of a free Mn^{4+} is 3.87 μ_B.

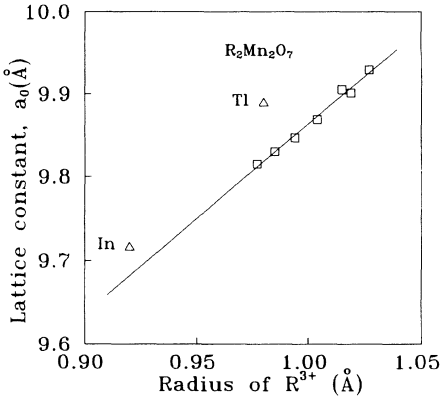

FIG. 1. Lattice constants of $R_2Mn_2O_7$ (R =Dy–Lu,Y □; R =In,Tl △) against radius of R^{3+}.

B. Magnetic data

Magnetic data of samples 1 and 2 of $Tl_2Mn_2O_7$ are found to be identical, so the data presented here are valid for both samples. Zero-field-cooled (ZFC) and field-cooled (FC) susceptibilities, obtained at an applied magnetic field of 50 G, are plotted against temperature in Fig. 2. There is no appreciable difference between ZFC and FC susceptibilities. These susceptibilities rise sharply below 140 K, and the magnetic ordering temperature is determined as 121±1 K from the inflection point. Inverse susceptibility against temperature is also given in Fig. 2. Data above 200 K are found to obey the Curie-Weiss law

$$\chi=\frac{C}{T-\Theta_p} . \tag{1}$$

From the Curie-Weiss plot the paramagnetic Curie temperature Θ_p is found to be +155 K indicating strong ferromagnetic exchange interactions between Mn moments. The Curie constant C is 1.96(3) emu K/mole of Mn ions and gives an effective paramagnetic moment P_{eff} of 3.96(3) μ_B/Mn. This is greater than the value of 3.87μ_B expected for a free Mn^{4+} ion. However, one should exercise caution in interpreting values derived from the Curie-Weiss analysis as the temperature range utilized, 200–300 K, is relatively limited compared with a T_c of about 121 K. Somewhat more reliable in this case is the saturation magnetic moment (Fig. 3), which reaches a constant value of 3.16(2) μ_B per Mn ion above applied fields of 0.8 T.

These magnetic results can be understood on the oxygen deficiency model, $Tl_2Mn_2O_{7-x}$. This will introduce $2x$ number of Mn^{3+} ions on the Mn sublattice. Mn^{4+} with a $3d^3$ configuration has $S=\frac{3}{2}$ and a small orbital contribution so the upper limit for the saturation moment, $gS=3.00\ \mu_B$/ion. Mn^{3+}, $3d^4$, with $S=2$ gives an upper limit of 4.00 μ_B/ion. Assuming that the Mn^{3+} and Mn^{4+} moments are coupled ferromagnetically, the measured saturation moment gives $x=0.16$. Data from the paramagnetic region are also consistent with this result. Theoretical Curie constants for Mn^{4+} and Mn^{3+} are 1.87 and 3.00 emu K/mole, respectively, and give a value of $x=0.12$.

Ferromagnetism is common in mixed valence Mn^{4+}/Mn^{3+} oxides such as $La_{1-x}Sr_xMnO_3$ (Ref. 18) and the coupling is ascribed to the double exchange mechanism.[16,17] Double exchange occurs between Mn^{3+} and Mn^{4+} ions by simultaneous transfer of an electron from Mn^{3+} to O^{2-} and O^{2-} to Mn^{4+} without change in the orientation of spin. This leads to ferromagnetic couplin due to the intra atomic Hund's rule requirement.[16] Double exchange is also consistent with the electrical properties of $Tl_2Mn_2O_{7-x}$ as seen in Sec. III C to follow.

Magnetic susceptibility data for $In_2Mn_2O_7$, obtained at an applied magnetic field of 50 G, are shown in Fig. 4. Unlike $Tl_2Mn_2O_7$ there exists a clear difference between the ZFC and FC susceptibilities below an apparent T_c of about 120 K. This behavior is one signature of a spin-glass sytem but is only a necessary, but not sufficient, condition for spin glass behavior. The Curie-Weiss plot above 200 K gives $\Theta_p=150$ K, similar to $Tl_2Mn_2O_7$, and a Curie constant, $C=1.78$ emu K/mole of Mn ions which is lower than for the $Tl_2Mn_2O_7$ compound. From

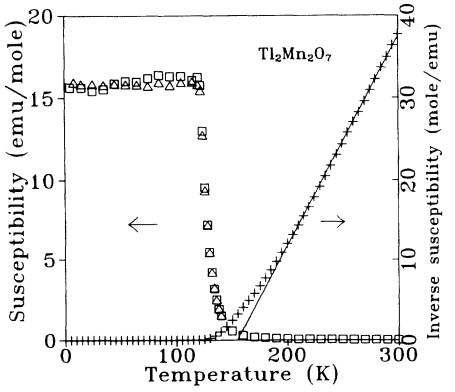

FIG. 2. ZFC (□), FC (△), and inverse (+) susceptibilities of $Tl_2Mn_0O_7$ against temperature obtained at an applied field of 50 G. Solid line represents Curie-Weiss fit to the data above 200 K.

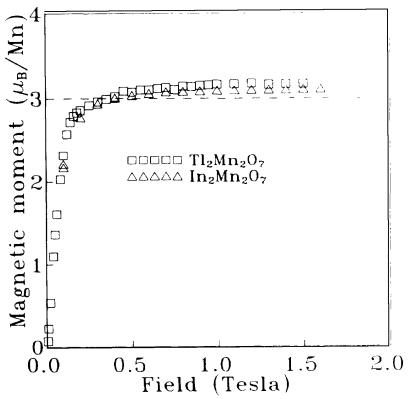

FIG. 3. Magnetic moment vs applied field for $Tl_2Mn_2O_7$ (□) and $In_2Mn_2O_7$ (△).

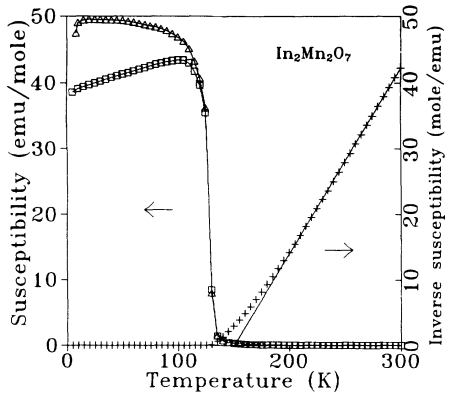

FIG. 4. ZFC (□), FC (△), and inverse (+) susceptibilities of $In_2Mn_2O_7$ against temperature obtained at an applied field of 50 G. Solid line represents Curie-Weiss fit to the data above 200 K.

Fig. 3 the saturation magnetic moment of $In_2Mn_2O_7$ is 3.10(2) μ_B/Mn. This suggests a slightly smaller Mn^{3+} content of $x=0.10$ for $In_2Mn_2O_{7-x}$ compared with $Tl_2Mn_2O_{7-x}$.

C. Electrical resistivity data

Electrical resistivity as a function of temperature is shown in Fig. 5 for sample 1 and sample 2 of $Tl_2Mn_2O_7$. Unlike the magnetic data, electrical resistivity behaviors of the two samples are different. However, both the samples show a very sharp drop in resistivity at the magnetic ordering temperature. If we consider the resistivity data above and below the ordering temperature (T_c), the data below T_c appear to behave similarly for both the samples with a small difference in their values. Above T_c, resistivity values differ by more than an order of magnitude. Room-temperature values of these two samples are compared with the literature value in Table I.

Sample 1 shows a very broad resistivity maximum centering around 200 K, similar to that of Ref. 13, and registers a sharp drop in resistivity upon crossing T_c.

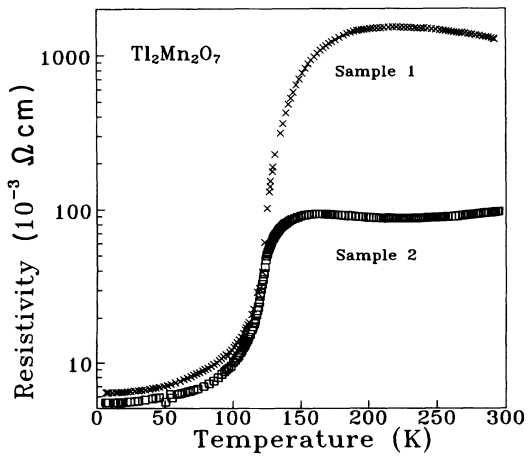

FIG. 5. Temperature variation of resistivity for sample 1 (×) and sample 2 (□) of $Tl_2Mn_2O_7$.

Whereas, the resistivity of sample 2 decreases with temperature down to about 200 K and then increases to a maximum around 150 K before it drops sharply. It was found in the mixed valence compounds $(La_{1-x}Sr_x)MnO_3$, that a marked decrease in resistivity occurs in the small temperature interval in which spontaneous magnetization develops.[18] This was attributed to the increase in the rate of electron transfer from Mn^{3+} to Mn^{4+} for those electrons with spins aligned parallel. Also the resistivity values are extremely sensitive to the ratio of Mn^{3+}/Mn^{4+} ions which appears to be the reason for different resistivity values for different samples of $Tl_2Mn_2O_7$.[19]

The room-temperature resistivity of $In_2Mn_2O_7$ is about 10^4 Ω cm falling between the values of $Tl_2Mn_2O_7$ (0.1–10 Ω cm) and $Y_2Mn_2O_7$ (10^6–10^8 Ω cm). This is also consistent with a smaller Mn^{3+} content in $In_2Mn_2O_7$ than in $Tl_2Mn_2O_7$.

D. SANS data of $Tl_2Mn_2O_7$

SANS is ideally suited for the study of microstructure in condensed matter on a length scale from a few atomic distances to about a few hundred angstroms, depending on a given instrument's resolution limits. Since the lattice constants and magnetic data of the two samples are in very good agreement, we have mixed sample 1 and sample 2 together in order to improve the SANS intensities. Figure 6(a) displays the temperature dependence of

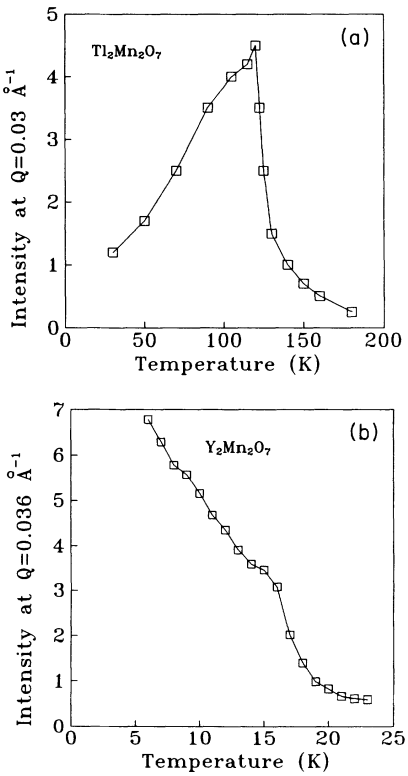

FIG. 6. (a) Small-angle neutron-scattering intensity (in arbitrary units) as a function of temperature at wave vector $Q=0.03$ Å^{-1} for $Tl_2Mn_2O_7$. Solid line is guide to the eye. (b) Small-angle neutron-scattering intensity (in arbitrary units) as a function of temperature at wave vector $Q=0.036$ Å^{-1} for $Y_2Mn_2O_7$. Solid line is guide to the eye.

the scattered neutron intensity at $Q=0.03$ Å^{-1}. The intensity increases with a decrease in temperature, reaches a cusplike maximum at T_c, and then decreases. This type of SANS behavior is expected for a ferromagnet because in a conventional ferromagnet, as the temperature is lowered towards T_c, the spin fluctuations develop a spatial coherence giving rise to the formation of magnetic clusters which tend to grow larger upon approaching T_c, and infinitely large with further decrease in temperature.[20]

Also for a ferromagnet, the Q dependence of the magnetic scattering obeys a Lorentzian profile

$$I(Q)=\frac{A}{Q^2+k^2}\ , \tag{2}$$

where A is a constant and k is the inverse of the spin correlation length ξ. The SANS data of $Tl_2Mn_2O_7$, over the Q range covered in the present studies, obey Eq. (2) as can be evidenced from the inverse intensity vs Q^2 plots in Fig. 7. In order to avoid over crowding of the data, we have provided two typical data sets one at 120 K, close to the T_c, and the other one at 140 K. Since the scattering intensity decreases rapidly above and below the T_c [see Fig. 6(a)], the scatter in the 140 K data set is more than that in the 120 K data set. At the phase transition, k goes to zero corresponding to an infinite spin correlation length $\xi=k^{-1}$. However, in actual practice instrumental resolution considerations limit the maximum measurable ξ to a few hundred angstroms. The spin correlation length ξ was determined by least-squares fitting of Eq. (2) to the experimental data. In Fig. 8 values of ξ are plotted against temperature. ξ increases rapidly below 130 K and reaches a resolution limited infinity (≈ 100 Å) at and below T_c suggesting a long-range order.

As mentioned in Sec. I, here we briefly compare and contrast the SANS results of $Tl_2Mn_2O_7$ with those of $Lu_2Mn_2O_7$ and $Y_2Mn_2O_7$. The behaviors of latter two materials were similar in most details and will be described in detail elsewhere.[6] Figure 6(b) shows SANS data at a similar Q-vector versus temperature for

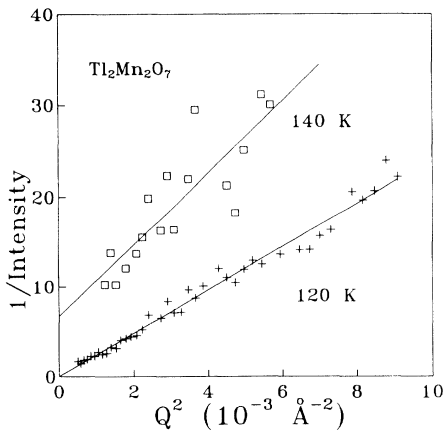

FIG. 7. Inverse scattering intensity (in arbitrary units) of $Tl_2Mn_2O_7$ vs Q^2 at 140 K (□) and at 120 K (+). Solid lines are the best fits to the Lorentzian profiles (see text).

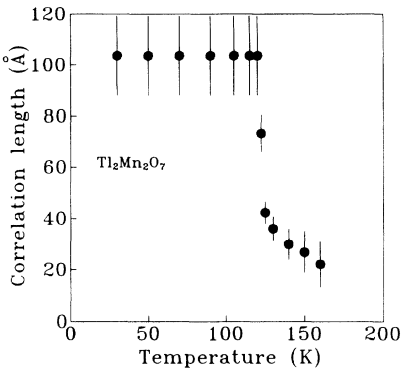

FIG. 8. Temperature dependence of spin correlation length ξ for $Tl_2Mn_2O_7$.

$Y_2Mn_2O_7$. Note the sharp rise in intensity beginning above 17 K which results in the cusp at 15 K. However, instead of falling as in $Tl_2Mn_2O_7$, the scattered intensity increases sharply as the temperature decreases. This effect is due to the presence of a Lorentzian squared term, $B/(Q^2+k_2^2)^2$, in the total cross section for $Y_2Mn_2O_7$, which arises from random field correlations, and Fig. 6(a) demonstrates the absence of this in the cross section for $Tl_2Mn_2O_7$.

A combination of the topology of the magnetic sublattice and the nearest-neighbor antiferromagnetic interactions are thought to be responsible for the suppression of long-range order in $Y_2Mn_2O_7$ and $Lu_2Mn_2O_7$. On this basis the long-range ferromagnetic ordering in $Tl_2Mn_2O_7$ implies that antiferromagnetic exchange interactions are either absent between Mn moments or extremely weak compared to ferromagnetic ones. The mixing of Mn^{3+} and Mn^{4+} on the magnetic sublattice could, via the double exchange mechanism, provide a sufficiently strong nearest-neighbor ferromagnetic interaction to result in long-range order.

E. Preliminary SANS data of $In_2Mn_2O_7$

In the present work, SANS intensities of $In_2Mn_2O_7$ are considerably weaker compared with those of $Tl_2Mn_2O_7$ due presumably to the high absorption cross section for In. A detailed analysis is thus precluded. However, the data at 120 K (close to T_c) where the SANS intensities are better are shown in Fig. 9. A linear plot of inverse intensity vs Q^2 reveals a Lorentzian profile. Also, a correlation length of about 105 Å has been determined from this plot. From the arguments put forward in the previous section, these findings, even though not extensive, suggest the possibility of long-range order in this material also. Experiments are planned to collect SANS data of better quality.

IV. SUMMARY

Magnetic susceptibility, electrical resistivity, and small-angle neutron-scattering measurements have been performed on the pyrochlore compounds $Tl_2Mn_2O_7$ and $In_2Mn_2O_7$ to study the nature of their magnetic ordering.

Magnetic phase transitions were observed at about 121 K from spontaneous magnetization. Saturation magnetic moments for $Tl_2Mn_2O_7$ and $In_2Mn_2O_7$ were found to be greater than the expected 3.0 μ_B/Mn^{4+}. This was attributed to the presence of Mn^{3+} ions on the B sublattice resulting from a small oxygen deficiency. The occurrence of spontaneous magnetization for $Tl_2Mn_2O_7$ and $In_2Mn_2O_7$ at high temperatures appears to arise due to the double exchange mechanism that couples Mn^{3+} and Mn^{4+} spins ferromagnetically. The same mechanism also explains the sharp drop in resistivity of $Tl_2Mn_2O_7$ around T_c. A cusplike maximum at T_c in SANS intensity vs temperature, the resolution limited spin correlation lengths at and below T_c, and the saturation moment of Mn spins clearly suggest a ferromagnetic long-range order in $Tl_2Mn_2O_7$. Topological considerations of the Mn sublattice indicate that *nn* antiferromagnetic interactions in this material are either absent or insignificant.

The magnetic data of the more insulating compound $In_2Mn_2O_7$ exhibit differences in ZFC and FC susceptibilities suggesting the possibility of a spin-glass nature. Nevertheless, the magnetic saturation behavior and the preliminary SANS data lend support to the presence of long-range order in this compound. Experiments are planned to measure the heat capacity of these materials which should provide conclusive evidence regarding the presence of long-range order.

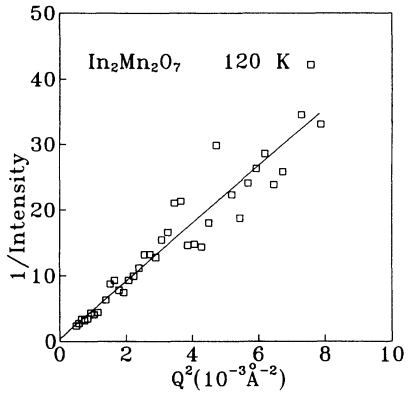

FIG. 9. Inverse scattering intensity (in arbitrary units) of $In_2Mn_2O_7$ vs Q^2 at 120 K (□). Solid line is the best fit to the Lorentzian profile (see text).

ACKNOWLEDGMENTS

We acknowledge the financial support of the Natural Science and Engineering Research Council of Canada and the Ontario Center for Materials Research. We thank J. Avelar for assistance with the SANS measurements and Professor C. V. Stager for the use of the SQUID magnetometer.

[1]M. A. Subramanian, G. Aravamudan, and G. V. Subba Rao, Mater. Res. Bull. **15**, 1401 (1980).

[2]P. W. Anderson, Phys. Rev. **102**, 1008 (1956); R. Liebmann, *Statistical Mechanics of Periodic Frustrated Ising Systems* (Springer, Berlin, 1986), p. 117; J. N. Reimers, A. J. Berlinsky, and A. C. Shi, Phys. Rev. B **43**, 865 (1991).

[3]M. A. Subramanian, C. C. Torardi, D. C. Johnson, J. Panetier, and A. W. Sleight, J. Solid State Chem. **72**, 24 (1988).

[4]J. N. Reimers, J. E. Greedan, R. K. Kremer, E. Gmelin, and M. A. Subramanian, Phys. Rev. B **43**, 3387 (1991).

[5]J. E. Greedan, J. Avelar, and M. A. Subramanian, Solid State Commun. **82**, 797 (1992).

[6]A. Maignan, Ch. Simon, J. E. Greedan, J. S. Pedersen, and M. A. Subramanian (unpublished).

[7]M. Sato, Xu Yan, and J. E. Greedan, Z. Anorg. Alig. Chem. **540/541**, 177 (1986).

[8]N. P. Raju, E. Gmelin, and R. K. Kremer, Phys. Rev. B **46**, 5405 (1992).

[9]K. Blacklock, H. W. White, and E. Gurmen, J. Chem. Phys. **15**, 1966 (1980).

[10]J. E. Greedan, M. Sato, X. Yan, and F. S. Razavi, Solid State Commun. **59**, 895 (1986).

[11]J. E. Greedan, J. N. Reimers, C. V. Stager, and S. L. Penny, Phys. Rev. B **43**, 5682 (1991).

[12]B. D. Gaulin, J. N. Reimers, T. E. Mason, J. E. Greedan, and Z. Tun, Phys. Rev. Lett. **69**, 3244 (1992); Guo Liu and J. E. Greedan (unpublished).

[13]H. Fujinaka, N. Kinomura, M. Koizumi, Y. Miymoto, and S. Kume, Mat. Res. Bull. **14**, 1133 (1979).

[14]I. O. Troyanchuk and V. N. Derkachenko, Fiz. Tverd. Tela. **30**, 3487 (1988) [Sov. Phys. Solid State **30**, 2003 (1988)].

[15]R. D. Shannon, Acta Cryst. A **32**, 751 (1976).

[16]C. Zener, Phys. Rev. **82**, 403 (1951).

[17]P. G. DeGennes, Phys. Rev. **118**, 141 (1960).

[18]G. H. Jonker, Physica **22**, 707 (1956); E. O. Wollan and W. C. Koehler, Phys. Rev. **100**, 545 (1955).

[19]J. H. Van Santen and G. H. Jonker, Physica **16**, 599 (1950).

[20]J. J. Rhyne and G. E. Fish, J. Appl. Phys. **57**, 3407 (1985).